[13]This value is in good agreement with that determined from the resistivity by using a hole mobility $\mu_h = 400$ cm^2 V^{-1}sec^{-1} [see J. Black, E. M. Conwell, L. Seigle, and C. W. Spencer, J. Phys. Chem. Solids 2, 240 (1957)].

[14]T. C. Harman, S. E. Miller, and H. L. Goering, J. Phys. Chem. Solids 2, 181 (1957).

[15]K. L. Shaklee, F. H. Pollak, and M. Cardona, Phys. Rev. Letters 15, 883 (1965).

[16]Preliminary results have already been presented [A. Balzarotti and P. Picozzi, Bull. Ital. Phys. Soc. 62, 83 (1968)].

[17]D. E. Aspnes and A. Frova, Solid State Commun. 7, 155 (1969).

[18]J. Feinleib, Phys. Rev. Letters 16, 1200 (1966).

[19]The reflectivity data were extrapolated to infinite energies by assuming a tail function $R = c(\hbar\omega)^{-\gamma}$ and γ was determined such that the phase angle $\chi = 0$ below the absorption edge [see, e.g., W. J. Scouler, Phys. Rev. 178, A1353 (1969)]. A value of $\gamma = 3.9$ was found to hold for the data of Ref. 11.

[20]I. G. Austin, Proc. Phys. Soc. (London) 72, 545 (1958).

[21]J. E. Fischer and B. O. Seraphin, Solid State Commun. 5, 973 (1967).

[22]F. Lukes, data cited in Ref. 21.

[23]S. Ballarò, A. Balzarotti, and V. Grasso, Phys. Status Solidi 28, K109 (1968).

[24]A. Balzarotti and M. Grandolfo, Solid State Commun. 6, 815 (1968).

[25]E. Schmidt and W. H. Knausenberger, J. Opt. Soc. Am. 59, 857 (1969).

[26]In the 1–3 eV region the pseudo-Brewster angle of Bi_2Te_3 was calculated by differentiating the Fresnel formula for R_p with respect to the angle of incidence. The values of φ_B range from about 74° at 3 eV to 84° at 1.0 eV. The introduction of the refractive index of the first medium ($n = 1.33$) moves φ_B to low energies of ~4° in this energy range.

[27]D. E. Aspnes and M. Cardona, Phys. Rev. 173, 714 (1968).

[28]A. Frova, P. J. Boddy, and Y. S. Chen, Phys. Rev. 157, 700 (1967).

[29]D. E. Aspnes, Phys. Rev. 153, A972 (1967).

[30]D. L. Greenaway, G. Harbeke, F. Bassani, and E. Tosatti, Phys. Rev. 178, 1340 (1969).

[31]Around 2.5 eV the effect of a strong anisotropy along the c axis of the optical constants on the R_p reflectance is to increase φ_B by about 3° and to enhance R_p by less than 5% for $\varphi < \varphi_B$ with respect to the isotropic case.

[32]M. Cardona and D. L. Greenaway, Phys. Rev. 133, A1685 (1964).

PHYSICAL REVIEW B VOLUME 3, NUMBER 4 15 FEBRUARY 1971

Diffuse X-Ray Scattering in Fast-Neutron-Irradiated Copper Crystals*

J. E. Thomas,† T. O. Baldwin,‡ and P. H. Dederichs§
Solid State Division, Oak Ridge National Laboratory, Oak Ridge, Tennessee 37830
(Received 15 June 1970)

Nearly perfect copper crystals with dislocation densities less than $\sim 10^3$/cm^2 have been irradiated with fast neutrons at doses up to 4×10^{19}/cm^2, and the diffuse x-ray scattering resulting from the defects produced has been studied in a variety of situations. Measurements were made with a double-crystal spectrometer to allow observations of the scattering very close (~ seconds of arc) to the Bragg peaks, for which a theoretical analysis of the data can be made. The diffuse scattering can be explained as resulting from defect clusters or dislocation loops ~100 Å in diam; there is an asymmetry of the diffuse scattering which appears to result from a predominance of large interstitial loops. This interpretation is consistent with electron-microscopy observations on these crystals. Diffuse scattering observations as well as anomalous x-ray transmission studies on irradiated crystals are suggested as very valuable tools to study the possibility of clustering phenomena in the annealing stages of various irradiated crystals.

INTRODUCTION

The irradiation of metal crystals is known to have marked effects on their physical properties. However, with the exception of lattice parameter measurements, little is known in a quantitative sense about the effects of irradiation on x-ray-diffraction properties. Although several years ago it was predicted that irradiation ought to cause strong diffuse scattering, [1] few observations of this scattering were made until quite recently in diamond, [2] copper, [3] silicon, [4] LiF, [5] BeO, [6] etc.

Diffuse x-ray scattering caused by the strains associated with radiation-induced defects in metals is quite difficult to observe for several reasons: (i) The diffuse scattering from point defects should be relatively weak for concentrations less than ~10^{19}/cm^3. If point defects are formed, as from electron irradiation, these defects are usually free to migrate at room temperature; hence, large doses of electron irradiation would be necessary at low temperatures to see the effects with conventional x-ray-diffraction apparatus (see, e.g., Simmons and Balluffi[7]); (ii) If clusters of defects

are formed, as from fast-neutron irradiation at reactor ambient temperatures, the diffuse intensity is very much enhanced but is located very near the Bragg reflections; thus, higher-resolution techniques than those conventionally used to observe thermal diffuse scattering or short-range-order effects (as in alloys) are necessary. (iii) Background corrections to the diffuse scattering are often difficult to make since standards often contain an unknown number of imperfections. These last two difficulties (low-resolution and background correction problems) can be eliminated by utilizing crystal-monochromatized radiation and single crystals of low dislocation density.

In previous studies on irradiated copper crystals,[3] a very intense diffuse scattering was observed near the Bragg reflections, and it was decided that an examination of this scattering in some detail was desirable, especially since corresponding electron-microscopy information and anomalous x-ray-transmission data existed on the defect configuration in these crystals. In this paper we present the diffuse-x-ray-scattering results obtained with the use of a double-crystal spectrometer on nearly perfect copper crystals which had been neutron irradiated, and compare the results with a kinematical theory applicable to small dislocation loops such as those observed in the electron microscope in these same crystals.

THEORY

The theory of diffuse scattering from defects which produce static displacements was first discussed by Ekstein[8] and Huang.[9] But in most theories only the results for isolated displaced atoms are discussed. More recently, Krivoglaz and Ryaboshapka[10] have considered the x-ray-scattering effects produced from small dislocation loops such as those previously observed in fast-neutron-irradiated copper. Their results are essentially applicable to our observations, and we employ some modifications of their theory in this paper. Details of the theory will appear in a later paper.[11]

Although the crystals used in this work were nearly perfect, it appears reasonable that a kinematical theory will apply to the diffuse intensity as normally used for thermal diffuse scattering, since most of the diffuse scattering is outside the range of the very narrow Bragg reflections. Hence, we use that approach in this paper, recognizing that very near the Bragg reflection a correction must be made for dynamical effects, and we discuss the consequences of this approximation later.

The intensity for diffuse scattering is given by

$$I_{\vec{k},\vec{k}'} = f_{\vec{K}}^2 S(\vec{K}) ,$$

where $\vec{k}$ is the incident wave vector, $\vec{k}'$ is the diffracted one, and $\vec{K} = \vec{k}' - \vec{k}$. The term $f_{\vec{K}}$ is the usual atomic-structure factor and $S(\vec{K})$ is the scattering function.

We will consider the scattering from interstitial clusters. We assume that we have N_{cl} clusters of radius R_{cl} and that each cluster contains n_{cl} interstitials. For small concentrations, $S(\vec{K})$ is then equal to N_{cl} times the square of a "cluster form factor"[11]:

$$S(\vec{K}) = N_{cl} \left| e^{i\vec{h}\cdot\vec{R}^I} \rho(\vec{q}) + g_{\vec{h}}(\vec{q}) \right|^2 , \tag{1}$$

with

$$g_{\vec{h}}(\vec{q}) = \int (d\vec{r}/V_c)\, e^{i\vec{q}\cdot\vec{r}} \left(e^{i\vec{h}\cdot\vec{t}(\vec{r})} - 1\right) . \tag{2}$$

Here $\vec{h}$ is a reciprocal-lattice vector, $\vec{q}$ is in the first Brillouin zone (and assumed to be "small" in the following), so that $\vec{K} = \vec{h} + \vec{q}$. The first term of Eq. (1) is the Fourier transform ρ of the interstitial density in a cluster, whereas the second term describes the scattering at the displaced lattice atoms. Here $\vec{t}(\vec{r})$ is the cluster-displacement field and V_c is the volume of the unit cell.

For $|q| \lesssim 1/R_{cl}$ we have $\rho \cong n_{cl}$ and similarly $g_{\vec{h}} \sim n_{cl}$ which is due to the "coherent" action of all the interstitials of the same cluster. For larger q values, ρ and g decrease rapidly. Therefore, we get strong intensities only for small $|q| \sim 1/R_{cl}$. Whereas for $\vec{h} = 0$ (small-angle scattering) both ρ and g are of the same order of magnitude; for $\vec{h} \neq 0$ (near Bragg reflections), g is much larger than ρ and determines the scattering alone.

Furthermore, $S(\vec{K})$ can be split into two parts, being symmetrical and antisymmetrical with respect to $\vec{q}$:

$$S(\vec{K}) \equiv S_{\vec{h}}(\vec{q}) = S_{\vec{h}}^s(\vec{q}) + S_{\vec{h}}^a(\vec{q}) . \tag{3}$$

For $|q| \ll 1/R_{cl}$ the symmetrical part goes $\sim N_{cl} n_{cl}^2 (h/q)^2$, whereas $S^a \sim 1/q$. S^s and S^a are also symmetrical and antisymmetrical functions with respect to the displacement field $\vec{t}(\vec{r})$. This means the asymmetry of the diffuse scattering depends upon the type of defect present leading to more intensity for higher Bragg angles in the case of interstitial-type defects and more intensity for lower Bragg angles in the case of vacancies.

In our particular geometry, rocking curves were measured with a wide-open counter; hence, we must integrate these expressions over $\vec{k}'$ along the Ewald sphere surface. For a rocking angle $\delta\theta$, we find that

$$I_0^s(\delta\theta) \sim N_{cl} R_{cl}^4 \lambda^2 \ln \left| \frac{\kappa}{q_0} \right| \quad \text{and} \quad I_0^a(\delta\theta) \sim \left| \frac{q_0}{\kappa'} \right| \ln \left| \frac{\kappa'}{q_0} \right| , \tag{4}$$

where $q_0 = \delta\theta h \cos\theta_B$. The terms I_0^s and I_0^a become the symmetrical and asymmetrical "integrated"

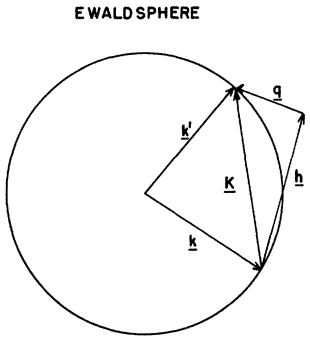

FIG. 1. Ewald sphere in reciprocal space; $\vec{k}$ is the incident-beam vector, $\vec{k}'$ is the diffracted-beam vector, and $\vec{h}$ is the reciprocal-lattice vector.

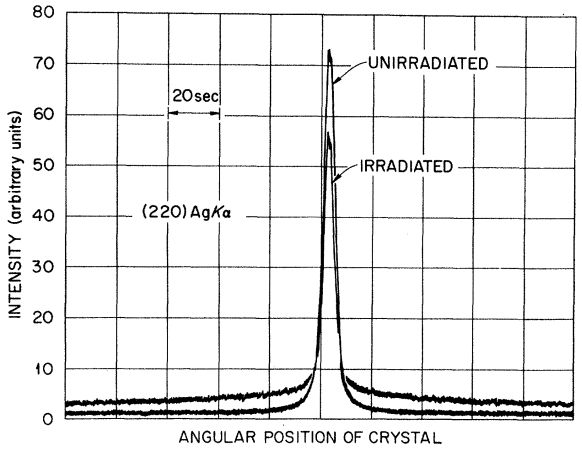

FIG. 2. The 220 Ag$K\alpha$ Bragg reflections for unirradiated and irradiated crystals. The fast-neutron dose was about $4\times10^{19}/\mathrm{cm}^2$ ($E>0.6$ MeV).

intensities, respectively. These, however, are not the usual integrated intensities, i.e., the area beneath the rocking curve, [5] but refer only to the total intensity received for each particular crystal setting. Hence, we see that a plot of I_0^s vs $\ln 1/q_0$ yields an intercept with the horizontal axis of κ which is $\approx 1/R_{cl}$, i.e., the reciprocal of the cluster or loop radius. In this analysis, no distinction can be made between clusters or loops; information in the asymptotic region "far" removed from the Bragg peaks must be utilized. However, it is just this region where the integral in Eq. (2) becomes difficult to evaluate owing to the large displacements $\vec{t}(\vec{r})$ from dislocation loops. Furthermore, Eq. (4) applies well only for relatively small values of the Bragg angle θ.

EXPERIMENTAL

The crystals studied here had been examined in detail previously in comprehensive anomalous x-ray-transmission studies. [3] Before irradiation, the diffracted-x-ray intensities in the Bragg and anomalous transmission geometries were essentially equivalent to those for perfect crystals, and several of these unirradiated crystals were used as "standards" to determine the background (Compton, thermal diffuse scattering, etc.) corrections necessary for the absolute diffuse-scattering-intensity measurements. Measurements of the incident-beam intensities were made with calibrated filters.

The crystals used were $1\times1\times t_0$ cm lamellae, where $0.05\ \mathrm{cm} < t_0 < 0.2\ \mathrm{cm}$, and they had (111), (100), (110), or (112) faces. Fast-neutron irradiation took place in the LITR reactor at Oak Ridge at about 40 °C with doses varying from 1.4×10^{18} to 4.2×10^{19} fast neutrons/cm^2 ($E>0.6$ MeV); the samples were shielded from thermal neutrons with cadmium.

After irradiation the crystals were etched in HNO_3 and then electropolished until smooth surfaces were obtained. Additional etching and polishing did not produce any changes in the results.

Diffuse-scattering measurements in the Bragg geometry were made with a double-crystal spectrometer in order to obtain measurements within seconds of arc of the Bragg peaks. Effectively, double-crystal rocking curves measure the integrated diffuse scattering, i.e., integrated over $\vec{k}'$ along the surface of the Ewald sphere in reciprocal space (see Fig. 1). Because most of the diffuse scattering is located so near the Bragg reflection, the differential diffuse scattering is substantially more difficult to measure and is not presented here.

RESULTS AND DISCUSSION

Figures 2 and 3 show rocking curves of 220- and

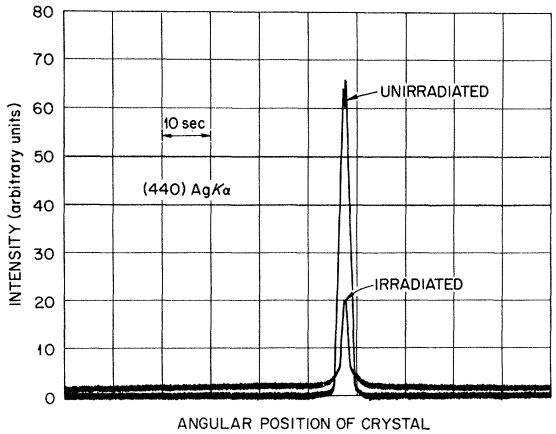

FIG. 3. As in Fig. 2 except that 440 Ag$K\alpha$ emphasizes the pronounced decrease in Bragg intensity and the "narrowing" of the half-width due to the static Debye-Waller factor $L_{\vec{n}}$ (consistent with text).

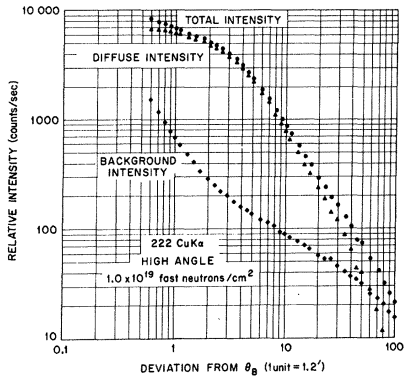

FIG. 4. Curves obtained for a 222-Cu$K\alpha$ reflection from a crystal irradiated with 1.0×10^{19} fast neutrons/cm^2, on the high-angle side of the Bragg peak. The background intensity refers to an unirradiated crystal. The incident-beam intensity was 304 000 counts/sec and 1.0 unit on the abscissa corresponds to 1.2 min. of are in $\delta\theta$.

440-Ag$K\alpha$ reflections, respectively, from a crystal irradiated with about 4×10^{19} fast neutrons/cm^2. The general features of these curves are the following: (a) The Bragg peaks are decreased in intensity and somewhat narrower than those for the perfect crystal. This result is much more apparent in the 400 than in the 220 reflection. (b) Very intense diffuse scattering appears in the wings of the Bragg peak within ~ 30 minutes of arc of the peak. Outside of this range the background intensity from the irradiated crystal is about that of the unirradiated crystal. (c) The total integrated intensity (Bragg + diffuse) is greater than that for the perfect crystal by a factor of 2 or more.

Figures 4–7 show the diffuse scattering associated with 111-type diffraction planes examined using both Cu$K\alpha$ and Mo$K\alpha$ radiation. As expected,

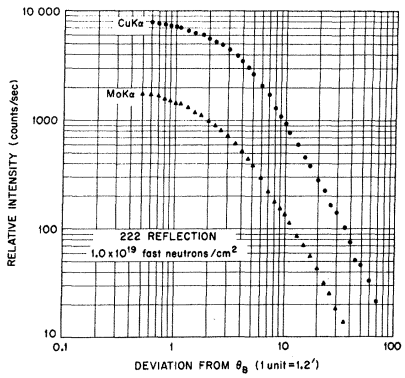

FIG. 5. 222 Cu$K\alpha$ and Mo$K\alpha$ diffuse intensity obtained on the same crystal; hence, this set of curves shows the λ^2 dependence of the diffuse scattering. The incident-beam intensity in each case was 362 000 counts/sec.

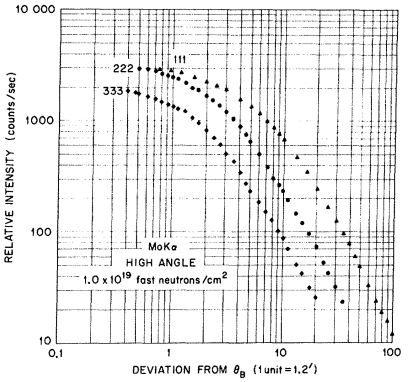

FIG. 6. Diffuse intensities near the 111, 222, and 333 reflections. The incident-beam intensity in each case was 605 000 counts/sec.

the absolute diffuse scattering varies nearly as λ^2 (Fig. 5). The way in which the diffuse scattering intensity varies with reflection (i.e., $\vec{h}$) is shown in Fig. 6. The data obtained from 200 and 220 reflections show essentially the same structure and, hence, are not presented here. Figure 7 shows the diffuse scattering for different fast-neutron

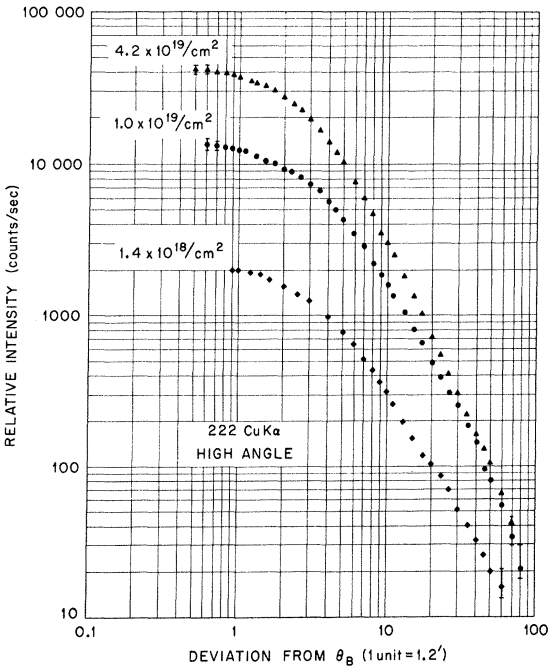

FIG. 7. Set of 222-Cu$K\alpha$ curves for crystals irradiated with fast-neutron doses of 1.4×10^{18}/cm^2, 1.0×10^{19}/cm^2, and 4.2×10^{19}/cm^2, respectively. These curves demonstrate that the diffuse scattering increases almost linearly in this range of dose. The incident-beam intensity was 812 000 counts/sec.

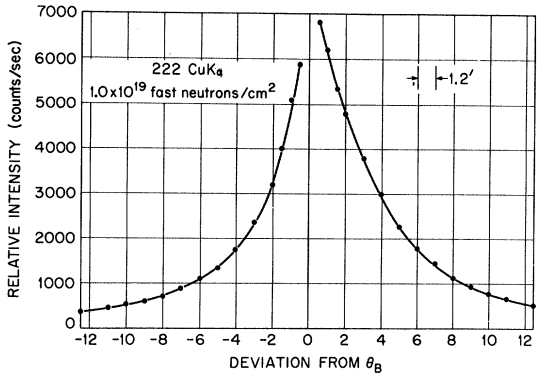

FIG. 8. Linear plot of the net diffuse scattering on both sides of the Bragg peak for the crystal in Fig. 4. The asymmetry suggests more large interstitial-type clusters are present. Note that the diffuse-scattering intensity is weighted toward large-size clusters [Eq. (4)].

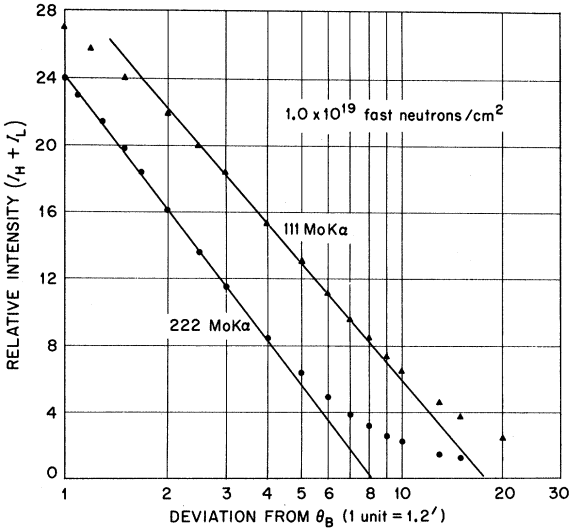

FIG. 9. Plot of intensity $I_0^s = I_{low} + I_{high}$ (where low and high refer to the two sides of Bragg peak) vs $\ln q_0$, Eq. (4). The intercept of the straight line with the abscissa yields $q \sim 1/R_{cl}$ and gives a measure of the cluster radius.

doses for a 222-Cu$K\alpha$ reflection. The latter indicates that the diffuse intensity is nearly linear with dose as one might expect from a linear increase in the concentration of loops with little or no change in the loop distribution. Some evidence of "saturation" begins to appear at the highest dose of 4.2×10^{19} fast neutrons/cm^2. The results deduced from these diffuse-scattering measurements are in general accord with those obtained using anomalous x-ray transmission.[12]

Figure 8 shows on a linear scale the observed asymmetry associated with these clusters of defects. As follows from the theory, this asymmetry toward larger Bragg angles could be expected to arise from a predominance of large interstitial loops.

From Eq. (4) we can deduce an effective radius for the clusters from the diffuse-scattering data. A plot of I_0^s vs $\ln q_0$ for small q_0 (Fig. 9) yields a radius which is determined by the intercept of the straight-line segment of the curve with the abscissa, i.e., $R_{cl} \approx d/2\pi \cos\theta\ (\delta\theta_i)$. The results obtained for Mo$K\alpha$ 111 and 222 gave $R_{cl} \approx 55$ and 61 Å, respectively. For larger q, i.e., for $|q| \geq 1/R_{cl}$, the slope of the log intensity vs log angular deviation from θ plots, as seen from Figs. 4–7, appears to be about two or perhaps slightly greater.

Another and perhaps better way to obtain information regarding cluster size is from the static Debye-Waller factor $L_{\vec{h}}$ for clusters or loops[10,12] which can be obtained by two methods: (i) from the decrease in Bragg integrated intensity $R_{H_I}/R_{H_U} = e^{-L_{\vec{h}}}$ (i.e., dynamical theory, neglecting diffuse wings) and (ii) from the integrated diffuse scattering [i.e., the area under the diffuse curves which yields directly $1 - e^{-2L_{\vec{h}}}$ (kinematical theory)].[13] These results should agree with the values found previously for $L_{\vec{h}}$ from anomalous transmission.

The results for a crystal irradiated with 1.0×10^{19} fast neutrons/cm^2 are shown in Table I and are seen to be in satisfactory agreement. Using density data obtained from electron-microscopy observations on these crystals, one would calculate $R_{cl} \approx 40$ Å. Note that $L_{\vec{h}}$ should be independent of wavelength but some small differences were observed. This may be caused by dynamical diffuse-scattering effects or other uncertainties, such as the subtraction of background in the immediate vicinity of the Bragg peak.

The results obtained here should be compared with electron-microscopy observations made on these same crystals.[14] The asymmetry in the diffuse-scattering suggests that there are more large interstitial loops than there are large vacancy loops present in these crystals. Most of the larger resolved loops observed in electron-microscopy observations have been identified as interstitial in

TABLE I. Debye-Waller factors $L_{\vec{h}}$ for Cu crystal 633-2-10 irradiated 1×10^{19} fast neutrons/cm^2.

$L_{\vec{h}}$	Bragg scattering		Diffuse scattering[a]		Anomalous transmission
	Mo$K\alpha$	Cu$K\alpha$	Mo$K\alpha$	Cu$K\alpha$	Mo$K\alpha$
111	0.08	0.04	0.05	0.08	0.08
222	0.15	0.14	0.18	0.19	0.17
333	0.45		0.41		

[a]Diffuse-scattering values are obtained using $f_{111} = 21.5$, $f_{222} = 14.0$, and $f_{333} = 9.4$.

character, although the total concentration of vacancies and interstitials appears to be about the same. However, the approximately linear increase in the diffuse-scattering intensities with dose is inconsistent with electron-microscopy results; the latter suggests that the concentration of loops begins to "saturate" at doses above $\sim 10^{19}/\text{cm}^2$ fast neutrons. Overlapping strain fields and a superposition of images in electron micrographs make a resolution of this apparent discrepancy difficult. The apparent cluster size of 55–60 Å agrees reasonably well with the results obtained previously using anomalous x-ray transmission. It should be pointed out, however, that whenever a distribution of loops is present, the larger loops play a dominant role in determining the diffuse intensities through the R_{cl}^4 dependence, which for a distribution of loops becomes the fourth moment. Hence, a size measured from the x-ray data will usually be considerably greater than the mean size as measured from electron micrographs.

DIFFUSE SCATTERING VERY NEAR BRAGG REFLECTION

Throughout this paper, it has been assumed that the diffuse scattering can be represented by the kinematical theory. Yet, in these nearly perfect crystals, the scattered intensities are represented by the dynamical theory at the Bragg reflections. The extent to which the theory presented here must be corrected at the Bragg reflection has not been calculated, but an attempt to measure this dynamical influence on the diffuse intensities has been made.

Batterman[15] and Annaka *et al.*[16] have shown in several papers that fluorescence, thermal diffuse scattering, and Compton scattering all show a minimum when Bragg conditions are met in nearly perfact crystals. This effect occurs because the incident beam is nearly totally reflected and hence, does not penetrate far into the crystal (i.e., the penetration is of order an extinction distance, rather than an absorption distance, as in the kinematical case for imperfect crystals). In the present case, one would expect that the incident beam would "see" fewer defects when Bragg conditions are met. To demonstrate this effect, it was necessary to shield the diffuse scattering from the Bragg reflection; this was done by placing a sharp edge on the high-angle side of the 220-Cu$K\alpha$ peak. The results obtained when the crystal was rocked through the Bragg angle are shown in Fig. 10. Although the minimum was clearly visible and coincident with the Bragg peak, it was not possible to measure quantitatively the intensities in the wings of the minimum which would demonstrate the different absorption characteristics of the two wave fields present (see, e.g., Refs. 15 and 16). However, from the present measurements, it would appear

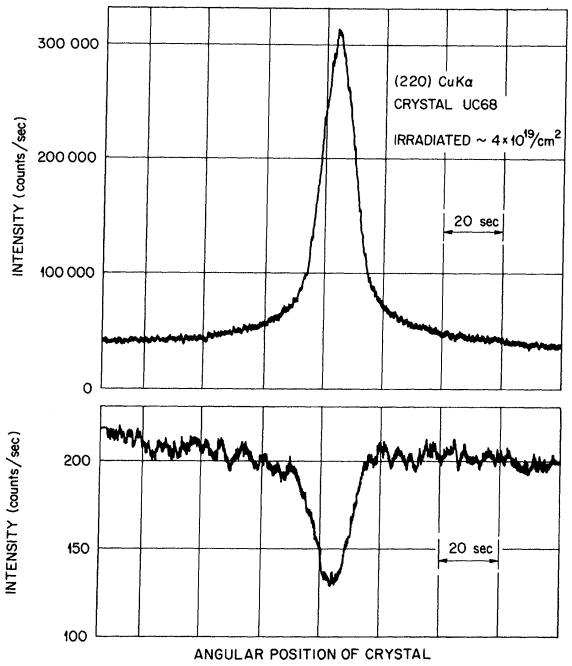

FIG. 10. The 220-Cu$K\alpha$ Bragg peak (top curve) and the corresponding diffuse-scattering minimum (just off the Bragg peak) as the crystal is rocked through the Bragg angle. (The upper curve was taken with calibrated filters to reduce the intensity to the linear limits of the detection system.) These curves demonstrate the dynamical diffuse-scattering effects present when the Bragg conditions are met.

that one must exercise great caution in applying the present theory very near Bragg reflections.

SUMMARY

Clearly, in heavily irradiated crystals, diffuse x-ray scattering can be used to obtain information regarding cluster sizes, types, and distributions. Fairly strict experimental limitations exist, in that nearly perfect crystals must be used if information is to be obtained very near the Bragg reflections. In the case of copper irradiated with fast neutrons, most of the diffuse scattering is contained within ~ 30 minutes of the Bragg peaks. In imperfect crystals, these results would be superimposed upon the "mosaic spread" of the crystal and, in effect, obscured. Information outside of this range of scattering angles is difficult to obtain due both to the smaller intensities and to the more complicated theoretical expressions. Nevertheless, in view of work by Bachmann *et al.*,[17] it appears that metal crystals with dislocation densities $\sim 10^5/\text{cm}^2$ would be satisfactory for these measurements.

As first pointed out by Patel and Batterman[18] in silicon, clustering phenomena can produce very

large effects on anomalously transmitted intensities, and similar results were found for irradiated copper.[3] When defects are clustered, changes in the x-ray-diffraction properties are produced with a relatively small number of point defects. In fact, diffuse x-ray-scattering measurements as those presented here would appear to be valuable in determining whether isolated point defects had, in fact, clustered after some treatment. These results as well as those obtained previously using anomalous x-ray transmission should be less ambiguous than electrical resistivity or lattice-parameter measurements, and a comparison with measurements of other physical properties would appear to be very useful in determining, for example, if clustering were important in low-temperature annealing stages. Such experiments are now being planned for some of these crystals.

ACKNOWLEDGMENT

The authors would like to express their appreciation to F. W. Young, Jr., for supplying the copper crystals used in these studies and for his continued encouragement and helpful discussions.

*Research sponsored by the U. S. Atomic Energy Commission under contract with Union Carbide Corp.

†Permanent address: Kansas State College, Pittsburg, Kans.

‡Permanent address: Southern Illinois University, Edwardsville, Ill. 62025.

§Visiting scientist from Technische Hochschule, Aachen, Germany.

[1]W. Cochran and G. Kartha, Acta Cryst. 9, 941 (1956).

[2]R. G. Perret and D. T. Keating, in *Small Angle X-Ray Scattering*, edited by H. Brumberger (Gordon and Breach, New York, 1967), p. 373.

[3]T. O. Baldwin, F. A. Sherrill, and F. W. Young, Jr., J. Appl. Phys. 39, 1541 (1968).

[4]R. Colella and A. Merlini, Phys. Status Solidi 14, 81 (1966).

[5]H. Peisl, H. Spalt, and W. Waidelich, Phys. Status Solidi. 23, K75 (1967).

[6]S. R. Austerman and K. T. Miller, Phys. Status. Solidi 11, 241 (1965).

[7]R. O. Simmons and R. W. Balluffi, J. Appl. Phys. 30, 1249 (1959).

[8]H. Ekstein, Phys. Rev. 68, 120 (1945).

[9]K. Huang, Proc. Roy. Soc. (London) A190, 122 (1947).

[10]M. A. Krivoglaz and K. P. Ryaboshapka, Phys. Metals Metallog. 15, 14 (1963).

[11]P. H. Dederichs (unpublished).

[12]F. W. Young, Jr., T. O. Baldwin, and P. H. Dederichs, in *International Conference on Vacancies and Interstitials in Metals*, edited by D. Schumacher (North-Holland, Amsterdam, 1968), Vol. II, p. 619.

[13]R. W. James, *Optical Principles of the Diffraction of X-Rays* (G. Bell and Sons, London, 1958).

[14]J. C. Crump, III (unpublished).

[15]B. H. Batterman, Appl. Phys. Letters 1, 68 (1962); Phys. Rev. 133, A759 (1964).

[16]S. Annaka *et al.*, J. Phys. Soc. Japan 21, 1559 (1966); 23, 372 (1967); 24, 1332 (1968).

[17]K. J. Bachmann, T. O. Baldwin, and F. W. Young, Jr., J. Appl. Phys. 41, 4783 (1970).

[18]J. R. Patel and B. W. Batterman, J. Appl. Phys. 39, 1541 (1968).

PHYSICAL REVIEW B VOLUME 3, NUMBER 4 15 FEBRUARY 1971

Electronic Structure of Disordered Systems

K. S. Dy*
Department of Physics, University of North Carolina, Chapel Hill, North Carolina 27514

and

Shi-Yu Wu†
Department of Physics, University of Louisville, Louisville, Kentucky. 40208

(Received 6 August 1970)

A method of calculating the electronic density of states in a disordered system is discussed. The case of bound bands is considered in detail. By a transformation of the overlap integral in the tight-binding theory, the Matsubara-Toyozawa and Matsubara-Kaneyoshi methods for calculating the electronic density of states is extended to topologically disordered systems. The same transformation is also applied to the band propagator expansion.

I. INTRODUCTION

In recent years, the problem of the effects of lattice disorder on the electronic density of states has been studied extensively.[1] The various techniques employed may be classified according to the types of disorder and the range of the electronic energy. It is customary to divide the electronic